





Article

Theoretical Model for the Prediction of Water Flux during the Concentration of an Olive Mill Wastewater Model Solution by Means of Forward Osmosis

Magdalena Cifuentes-Cabezas ¹, Silvia Álvarez-Blanco ^{1,2}, José Antonio Mendoza-Roca ^{1,2},
María Cinta Vincent-Vela ^{1,2} and José M. Gozávez-Zafrilla ^{1,2,*}

- ¹ Institute for Industrial, Radiophysical and Environmental Safety (ISIRYM), Universitat Politècnica de València, Camino de Vera s/n, 46022 Valencia, Spain; magcica@upv.es (M.C.-C.); sialvare@iqn.upv.es (S.Á.-B.)
² Department of Chemical and Nuclear Engineering, Universitat Politècnica de València, Camino de Vera s/n, 46022 Valencia, Spain
* Correspondence: jmgz@iqn.upv.es

Abstract: Currently, understanding the dynamics of the interaction between the agents in a process is one of the most important factors regarding its operation and design. Membrane processes for industrial wastewater management are not strangers to this topic. One such example is the concentration of compounds with high added value, such as the phenolic compounds present in olive mill wastewater (OMW). This process is a viable option, thanks to the forward osmosis (FO) process, osmotically driven by a saline stream. In this context, the transport of the solute and the solvent through the FO membranes, although essential to the process, remains problematic. This paper presents a study to predict, by means of a theoretical model, the water flux for two membranes (a cellulose triacetate flat sheet and a polyamide hollow fiber with integrated aquaporin proteins) with different characteristics using a sodium chloride solution as the draw solution (DS). The novelty of this model is the consideration of the contribution of organic compounds (in addition to the inorganic salts) to the osmotic pressure in the feed side. Moreover, the geometry of the modules and the characteristics of the membranes were also considered. The model was developed with the ability to run under different conditions, with or without tyrosol (the compound chosen as representative of OMW phenolic compounds) in the feed solution (FS), and was fitted and evaluated using experimental data. The results presented a variability in the model prediction, which was a function of both the membrane used and the FS and DS, with a greater influence of tyrosol observed on the permeate flux in the flat cellulose triacetate membrane.

Keywords: forward osmosis; modeling; tyrosol; olive mill wastewater; simulation



Citation: Cifuentes-Cabezas, M.; Álvarez-Blanco, S.; Mendoza-Roca, J.A.; Vincent-Vela, M.C.; Gozávez-Zafrilla, J.M. Theoretical Model for the Prediction of Water Flux during the Concentration of an Olive Mill Wastewater Model Solution by Means of Forward Osmosis. *Membranes* **2023**, *13*, 745. <https://doi.org/10.3390/membranes13080745>

Academic Editor: Hongjun Lin

Received: 28 July 2023

Revised: 17 August 2023

Accepted: 19 August 2023

Published: 21 August 2023



Copyright: © 2023 by the authors. Licensee MDPI, Basel, Switzerland. This article is an open access article distributed under the terms and conditions of the Creative Commons Attribution (CC BY) license (<https://creativecommons.org/licenses/by/4.0/>).

1. Introduction

Currently, industries are increasingly interested in applying technologies to treat their wastewater. This is due to the great scarcity of water in some areas, as well as the rigorous laws regarding discharges [1]. Specifically, in the Mediterranean area, olive oil production is one of the main agricultural activities. This industry generates a large amount of olive mill wastewater (OMW), with a high organic content and the presence of phytotoxic compounds [2]. Although the proposed treatment strategies are usually successful in recycling water and reducing the amount of wastewater, most treatment technologies consume large amounts of energy. Therefore, it is necessary to develop treatment techniques that manage to provide treatment in an energy-efficient manner. The recovery of compounds present in wastewater begins as a strategy to amortize wastewater treatment, since it is possible to obtain products with high profit from waste, promoting a circular economy [3]. In OMW, the phenolic compounds mainly provide its phytotoxic character. These compounds, besides being recalcitrant, possess outstanding antioxidant

properties. Among the phenolic compounds present in OMW, tyrosol is one of the major compounds, being recognized for its antioxidant, anti-inflammatory, and antimicrobial properties. Therefore, its recovery is of great interest for its future commercialization in cosmetic, food, and pharmaceutical industries [4].

Concentration processes, besides being part of the main operating units of many industrial sectors, either for the processing, obtaining, and/or extraction of products, have also been studied regarding the recovery of compounds and the treatment of wastewater. Among these, pressure-driven membrane processes are widely used in various applications. Although these processes offer several advantages over traditional technologies, such not requiring additives, to date, there is still no technology that offers a fully satisfactory solution that allows treatment with low energy cost [5]. Within membrane processes, forward osmosis (FO) has recently received a great deal of interest in wastewater treatment. This is due to the fact that, compared to membrane pressure processes, it exhibits a lower fouling potential and low energy consumption, allows for the simultaneous treatment of two currents in a single treatment step, and also enables the treatment of liquids that are not suitable for other membrane processes [6]. These characteristics of the FO process make it stand out from other phenolic compound concentration/recovery processes. Although good results have been obtained using direct contact membrane distillation (DCMD), in DCMD, it is necessary to maintain a $\Delta T = 30\text{ }^{\circ}\text{C}$ between the FS and the permeate, making the process more expensive [7], while the phenolic compounds may also be affected by the increase in temperature.

In FO, it is the concentration gradient (also called osmotic pressure difference, $\Delta\pi$) that acts as the driving force to generate a flow of water through the membrane, which requires little external energy. The process separates two streams, one with low osmotic pressure (feed solution, FS) and other with higher osmotic pressure (draw solution, DS), through a semi-permeable membrane. Due to the difference in osmotic pressure between both streams, water permeates from the FS side to the DS side of the membrane, thus concentrating the FS while simultaneously diluting DS [8]. In the case of OMW, the phenolic compounds are concentrated in this manner for subsequent recovery.

However, this FO process also presents some obstacles, such as reverse solute flux and concentration polarization (CP), leading to a decrease in FO efficiency. CP occurs near the membrane walls in FS and DS—a phenomenon called external concentration polarization (ECP). Nevertheless, it is a relatively less significant problem than internal concentration polarization (ICP) in the FO processes. ICP in the support layer represents a significant obstacle to the permeation of water through the membrane. The extracting solute penetrates the porous support layer of the membrane according to Fick's law. The diffused solute is then diluted with the water diffused from the FS to the support layer, generating a reduction in the osmotic pressure gradient across the active layer and therefore, a corresponding reduction in water flux [9,10]. However, as this is inherent to the membrane structure, result is difficult to mitigate [11].

On the other hand, more factors can influence the performance of the FO process, including membrane-specific factors (material, structure, surface area, and configuration), FS and DS characteristics, and operating parameters [12]. Therefore, as indicated by Singh et al. [13], understanding the dynamics of solute and solvent transport through osmotic-driven membranes, although essential, remains an unsolved problem at this time.

Different models have been developed to explain the fundamental process of FO, such as the early models of Lee et al. [14] and Loeb et al. [15], which considered a reverse solute flow, and this the version was later improved by Tang et al. [16], who including the concept of inverse solute selectivity, or the model of Suh and Lee [9], which considered ECP. However, although there has been further development and research regarding the FO process in recent years, there is still a scarcity of literature concerning modeling studies of the FO process. Some attempts have been made in regards to the treatment of phenolic compounds using FO [17,18]. To our knowledge, to date, there are no studies prior to this work considering FO modeling with OMW, with either real or simulated solutions.

The first models developed for the prediction of permeate flux in these processes were proposed by Ref. [14]. Although these models were the basis for understanding the FO process, they were developed for RO and PRO processes (reverse osmosis and pressure retarded osmosis). Then, it was the authors of [15] who transformed these models for use in FO. These authors were able to predict both the permeate flux and the reverse passage of the salts under a theoretical model that is still widely used today. However, these models are quite generic for analyzing the differences between the impact generated by both the salts in the draw solution and the components that are present in the feed. That is why these models, in spite of being the basis for understanding the FO process, must be modified and improved, according to the specific work characteristics. More recently, Ref. [19] performed additional studies regarding ICP (internal concentration polarization). However, as the authors of [20] point out in their work on the model prediction of flux behavior considering ECP (external concentration polarization) and ICP, at high DS concentrations (greater than 1.0 M NaCl) and high water fluxes, some theoretical models overestimate the flux of water across the membrane at the corresponding osmotic pressure. Therefore, they emphasize the need for a more accurate model for flux prediction, process optimization, fouling studies, treatment of potential feed streams, etc.

It is also very relevant to analyze different types of FS, considering that in the aforementioned studies [15,19], the feed and draw solutions used were deionized water and NaCl solutions. The NaCl concentrations varied from 0 (deionized water) to 1.0 M for FS and from 0.05 to 1.5 M for DS. Thus, more specific models must be developed. There are some considerations that could be taken into account for a best prediction of water flux in FO processes. Thus, Haupt et al. [21] analyzed three theoretical models for the modeling of the FO process for different types of wastewater from the automobile industry (cathodic dip painting rinsing water, cathodic dip painting wastewater, paint shop pre-treatment wastewater, and cooling tower circulation water). They concluded that, in some experiments, the permeate fluxes could be fitted to those predicted by the models, but in others, the water fluxes were overestimated or underestimated. They attributed this to the fact that fouling is not considered in the models, as well as to the complex composition structure of industrial wastewater, which may also influence the FO process. It is also important to note that, as the concentration process progresses, the effect of the composition of the feed on the driving force becomes more relevant. Some compounds show much greater rejection than others. These aspects are very important in a field such as the treatment of OMW in which different compounds are involved.

The aim of this study was to predict, by means of a theoretical model, the water flux of two membranes of different characteristics: a hollow fiber membrane of thin-film composite polyamide (TFC), integrating aquaporin proteins, and a flat-sheet membrane of triacetate of cellulose (CTA). This model has the ability to perform under different conditions, with or without tyrosol (the target phenolic compound of OMW) in the FS. The mathematical model takes into account mass balance, as well as membrane characteristics and concentration polarization equations. The model was fitted to and evaluated with data from a dynamic FO process. Two types of characterization tests were carried out, depending on the composition of the FS: (i) sodium chloride solutions and (ii) OMW model solutions (sodium chloride and tyrosol).

2. Theory

In FO, permeation is mainly influenced by the species making the greatest contribution to the chemical potential and consequently, to the osmotic pressure, such as low molecular weight salts. In the dense layer of an FO membrane, water flux is driven by the osmotic pressure difference associated with the solute concentrations in the FS and DS. For ideal conditions, the water flux (J_w) in an FO process is as follows [14,19]:

$$J_w = A_w \cdot \sigma \cdot (\pi_D - \pi_F) \quad (1)$$

where A_w is the membrane permeability coefficient, σ the reflection coefficient, and $\pi_D - \pi_F$ is the difference in osmotic pressure between the feed and draw solutions across the membrane selective layer. Assuming a perfect barrier, i.e., the salt does not cross the membrane, the reflection coefficient can be considered as equal to one.

External concentration polarization, defined as the increase or decrease in the solute concentration near the membrane surface with respect to the bulk solution, is common in any FO process and must be taken into account. However, most of the commercially available membranes are asymmetric, with a dense active membrane layer supported on a porous layer. In this case, internal concentration polarization, produced on the membrane support layer, can affect FO performance more significantly than ECP due to reverse salt diffusion from the DS towards the FS.

2.1. Transport Model for Asymmetric FO Membranes

Some studies neglect the salt concentration of the feed solution, but in this study, as in Refs. [14,19], it is considered. However, a novelty of our study is the consideration of the contribution to the osmotic pressure on the feed side of the organic compounds, in addition to that of the salt. The situation studied is shown in Figure 1, which shows the salt concentration profile through an asymmetric membrane, with a porous support layer and a dense active layer working in forward osmosis mode.

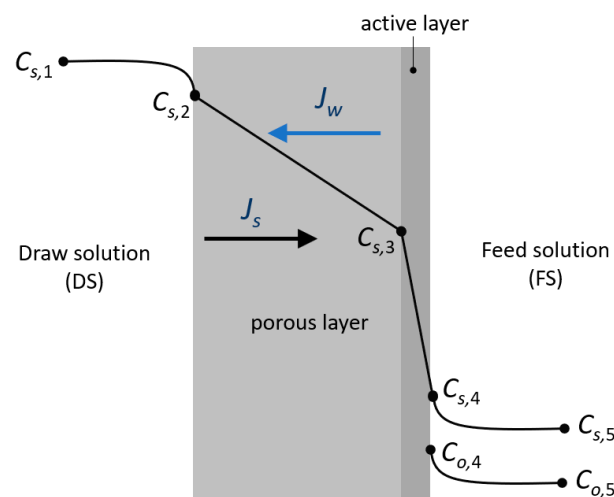


Figure 1. Concentration profiles across the membrane in forward osmosis mode for salt (s) and phenolic organic compounds (o).

According to film theory [20], the steady state concentrations in the bulk feed solution and at the membrane wall are related to the water flux and the transport coefficient of the components in each compartment:

$$J_w = -k_{sD} \cdot \ln \frac{C_{s,1}}{C_{s,2}} = -k_{sF} \cdot \ln \frac{C_{s,4}}{C_{s,5}} = -k_{oF} \cdot \ln \frac{C_{o,4}}{C_{o,5}} \quad (2)$$

The mass transport coefficients, $k_{i,j}$ in Equation (3), depend on the hydrodynamics of the draw (D) or feed (F) compartments and the solute characteristics. For a rectangular channel and turbulent flow, they can be obtained from a Sherwood (Sh) correlation (Equations (3) and (4)) taking into account the Reynolds (Re) and Schmidt (Sc) numbers [22]:

$$k = \frac{Sh \cdot D}{d_h} \quad (3)$$

$$Sh = 0.04 \cdot Re^{0.75} \cdot Sc^{0.33} \quad (4)$$

where D is the solute diffusivity in the solvent and d_h the hydraulic diameter of the membrane feed channel. The reverse salt flux (J_s) through the active layer of the membrane is given by the following equation:

$$J_s = B_s \cdot (C_{s,3} - C_{s,4}) \tag{5}$$

where B_s is the solute permeability coefficient, and $C_{s,3}$ and $C_{s,4}$ are the solute concentration in the draw and feed interfaces of the membrane active layer, respectively (see Figure 1).

The ICP profile in the porous layer is obtained using the convection–diffusion equation for the solute flux [15]:

$$J_s = -D_s \cdot \epsilon \cdot \frac{dC_s}{dx} - J_w C_s \tag{6}$$

The integration of Equation (6) in the porous layer between points 3 and 4 yields:

$$J_w = \frac{1}{K_s} \ln \left(\frac{J_w \cdot C_{s,3} + B_s \cdot (C_{s,3} - C_{s,4})}{J_w \cdot C_{s,4} + B_s \cdot (C_{s,3} - C_{s,4})} \right) \tag{7}$$

where K_s is the internal polarization modulus (Equation (8)), which depends on the diffusion coefficient of the salt (D_s) and a structural membrane parameter S (Equation (9)) calculated from the thickness (Δx), tortuosity (τ) and porosity (ϵ) of the porous support layer.

$$K_s = \frac{S}{D_s} \tag{8}$$

$$S = \frac{\tau \cdot \Delta x}{\epsilon \cdot D_s} \tag{9}$$

At a given temperature, it was assumed that the contribution to the osmotic pressure of each component in a position j is proportional to the component concentration through a constant osmotic coefficient (α), taking into account the modified van 't Hoff formula [23,24]:

$$\pi_j = \alpha_{s,j} \cdot C_{s,j} + \alpha_{o,j} \cdot C_{o,j} \tag{10}$$

Equation (10) was applied, without taking into account the osmotic contribution of the organic compounds for points $j = 1, 2, 3$ in Figure 1, but for the feed side (point 4) and the feed bulk (point 5), the osmotic contribution of other components, different from salt, was not neglected.

Applying Equation (1) to both sides of the active layer:

$$J_w = A_w \cdot (\pi_3 - \pi_4) = A_w \cdot (\alpha_s C_{s,3} - \pi_4) \tag{11}$$

where $C_{s,3}$ can be expressed as:

$$C_{s,3} = \frac{A_w \pi_4 + J_w}{\alpha_s A_w} \tag{12}$$

Therefore, the combination of the previous equations results in Equation (13), proposed for the numerical determination of the water flux, considering this osmotic contribution:

$$J_w = \frac{1}{K_s} \ln \left(1 - \frac{J_w \cdot (A_w \cdot (\pi_4 - \alpha_s C_{s,2}) + J_w)}{B_s \cdot (A_w \cdot (\pi_4 - \alpha_s C_{s,4}) + J_w) + A_w \pi_4 \cdot J_w + J_w^2} \right) \tag{13}$$

Once water flux is known, the salt flux can be calculated using:

$$J_s = B_s \cdot (C_{s,3} - C_{s,4}) = B_s \cdot \left(\frac{A_w \cdot \pi_4 + J_w}{\alpha_s A_w} \right) - C_{s,4} \tag{14}$$

To consider the effect of ECP, Equations (13) and (14) must be combined with Equation (2) to obtain the osmotic pressure at point 4 (feed side) from the information for the respective bulk concentrations (points 1 and 5) and the specific transport coefficients:

$$\pi_4 = \pi_{Fs} \exp\left(\frac{J_w}{k_{Fs}}\right) + \pi_{Fc} \exp\left(\frac{J_w}{k_{Fc}}\right) \tag{15}$$

$$\pi_2 = \pi_{Ds} \exp\left(-\frac{J_w}{k_{Ds}}\right) \tag{16}$$

Note that, in the absence of ECP, if the osmotic pressure is due exclusively to salt, then Equation (13) reduces to the commonly used equation, which McCutcheon and Elimelech [19] used to describe the FO process:

$$J_w = \frac{1}{K} \ln\left(\frac{A_w \pi_2 + B_s}{A_w \pi_4 + B_s + J_w}\right) \tag{17}$$

which can be used for initialization purposes during the parameter fitting.

2.2. Dynamic Model of the Forward Osmosis System

The FO system was modeled as two homogeneous compartments exchanging water and solutes across a membrane of area A . The osmotic pressure difference between the FS and DS is the driving force that causes the flow of water from the feed solution to the draw solution. Conversely, a small salt flux is received by the feed solution.

Assuming constant density, the balance equations for the feed and draw compartments, whose volume is represented by V , lead to the following ordinary differential equation system:

$$\frac{dV_D}{dt} = J_w \cdot A \tag{18}$$

$$\frac{dV_F}{dt} = -J_w \cdot A \tag{19}$$

$$\frac{dC_{D,s}}{dt} = (-J_s - J_w \cdot C_{D,s}) \cdot \frac{A}{V_D} \tag{20}$$

$$\frac{dC_{F,s}}{dt} = (-J_s - J_w \cdot C_{F,s}) \cdot \frac{A}{V_F} \tag{21}$$

$$\frac{dC_{F,c}}{dt} = (J_w \cdot C_{F,c}) \cdot \frac{A}{V_F} \tag{22}$$

where J_s and J_w are functions of the composition in both compartments, calculated using the most accurate transport model given by Equations (10)–(17).

3. Materials and Methods

3.1. Feed and Draw Solutions

For the experimental tests, model solutions were used on both membrane sides. For the FS, a tyrosol solution of $1 \text{ g}\cdot\text{L}^{-1}$ in distilled water was used. This concentration was selected, as it is similar to the total phenolic concentration measured in the characterization of an OMW obtained in a previous work [25]. Sodium chloride (VWR chemicals, Belgium), at concentrations of $30 \text{ g}\cdot\text{L}^{-1}$ and $200 \text{ g}\cdot\text{L}^{-1}$, was used for the DS. Both salt concentrations were selected because in other studies [26], they led to high permeate fluxes and low reverse salt fluxes. As for the $30 \text{ g}\cdot\text{L}^{-1}$ of NaCl concentration, this was selected based on the characterization of an actual brine obtained from the table olive producing industry [27].

3.2. Forward Osmosis Test

All the tests were carried out in FO in countercurrent flow, with the FS in front of the active layer of the membrane, due to its higher efficiency in terms of water flux and

fouling [28]. Two different membranes were tested, the FTSH2O™ flat sheet membrane (Fluid Technology Solutions, Albany, OR, USA), using the CFO42 module (Sterlitech Corporation, Auburn, WA, USA), and the HFFO2 hollow fiber membrane (Aquaporin Inside, Lyngby, Denmark), incorporated in its own module. The specific characteristics of each membrane are presented in Table 1. The fit of the proposed model was evaluated by comparing the simulated and experimental results. The effects of both concentrative ICP and dilutive ECP were investigated simultaneously.

Table 1. Characteristics and properties of the FO membranes.

Parameter	FTSH2O	HFFO2
Material	Cellulose triacetate	Polyamide with integrated aquaporin proteins
Configuration	Flat sheet	Hollow fiber
Area (m ²)	0.0042	2.3

First, a characterization of both membranes was carried out to obtain the specific parameters of each one (A_w , B_s and K_s). For this, different DS concentrations were used, all prepared with NaCl, in quantities ranging between 25 and 200 g·L⁻¹ (0.43 to 3.5 M, respectively), and pure water (conductivity < 40 μS·cm⁻¹). The operating conditions for the characterization tests were the same for both membranes, with flow rates of 25 L·h⁻¹ for the FS and 15 L·h⁻¹ for the DS. Then, two tests were carried out to evaluate the prediction of the selected model: (i) a test using distilled water as the FS and a concentration of 200 g·L⁻¹ of NaCl for the DS; and (ii) a test using 1 g·L⁻¹ of tyrosol as the FS and 30 g·L⁻¹ of NaCl as the DS (see [29] for the justification of the concentrations used). In the case of the FTSH2O membrane, the FS and the DS were pumped at a flow rate of 30 L·h⁻¹, while for the HFFO2 membrane, the experiments were carried out at 60 L·h⁻¹ for the FS and 25 L·h⁻¹ for the DS (based on manufacturer recommendations and previous studies carried out by the research group). The salt concentration was measured by means of conductivity, as well as using Merk kits (Darmstadt, Germany) measuring the ion Cl⁻. For the tyrosol concentration measurement, the Folin–Ciocalteu spectrophotometric method [30] was employed, using tyrosol as a standard (Maybridge, Altrincham, UK).

The permeate flux J_w was measured experimentally using the weight variation of the DS, as described in Equation (23), while the solute flux J_s was determined by considering the salt mass variation in the FS using Equation (24).

$$J_w = \frac{\Delta m}{A \cdot \Delta t} \tag{23}$$

$$J_s = \frac{V_t \cdot C_t - V_{t-1} \cdot C_{t-1}}{A \cdot \Delta t} \tag{24}$$

In the above equations Δm corresponds to the mass change of the draw solution, Δt is the time interval between the mass measurements, and C_t and V_t are the salt concentration and the volume of the feed solution, respectively, at time t .

Therefore, to model the behavior of an FO membrane, there are three parameters that fully describe its performance: water permeability (A_w), salt permeability (B_s), and a structural parameter (K_s), which is related to the internal polarization modulus K_s .

4. Results and Discussion

4.1. Model Parameter Determination

The main objective of the characterization of the membrane is to determine the value of the internal polarization modulus K . It is a parameter that depends mainly on the nature of the solute and the porous medium through which it diffuses; it should, therefore, be relatively constant for a given solute and membrane, whatever the value of J_w or $\Delta\pi$ [15].

Figures 2 and 3 show the experimental data and the fit obtained with the model. It can be seen that permeate flux increases upwards along with the increase in the concentration

of the DS solution. However, a pronounced non-linear trend is observed. McCutcheon and Elimelech [19] pointed out that a significant salt passage from the draw solution moves the representation of J_w versus the osmotic pressure difference away from linearity due to the presence of ICP. This may be due to the orientation of the membrane active layer (the FS faced the dense active layer), since in this orientation, the ICP effect predominates over the ECP effect. Therefore, a dilutive ECP and a concentrative ICP would result [13].

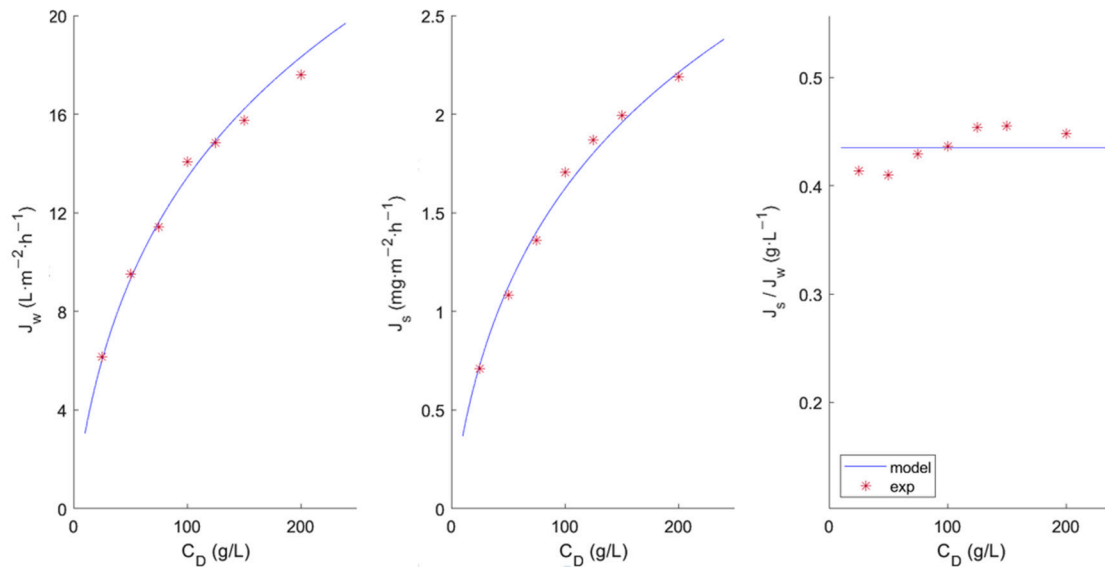


Figure 2. Characterization of the FTSH2O membrane by means of the water flux (J_w) and reserve salt passage (J_s) at different salt concentrations in the draw solution.

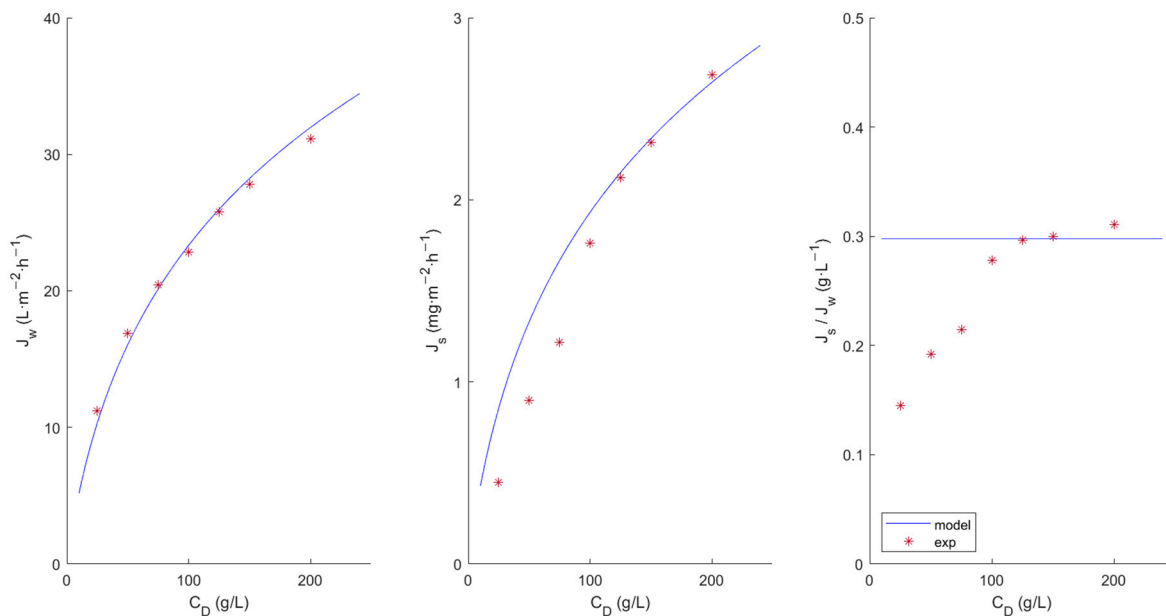


Figure 3. Characterization of the HFFO2 membrane by means of water flux (J_w) and reserve salt passage (J_s) at different salt concentrations in the draw solution.

Regarding the proposed model, the good fit of the model can be clearly observed for both membranes, predicting water fluxes at various SD concentrations close to the experimental value. However for the HFFO2 membrane (Figure 3), it seems to predict a higher salt flux than that observed at lower concentrations. This could be due to the fact that the membranes did not reach a stationary state, which would justify the ob-

served variation in J_s/J_w . Longer trials should be performed to study this phenomenon more precisely.

The results of A_w , B_s , and K_s for the HFFO2 (HF) and FTSH2O (FT) membranes are shown in Table 2. They were obtained by minimizing the quadratic error for J_w and J_s in the characterization test. To determine the values of these parameters, an initial calculation was carried out, without considering CP. Then, the model was applied in the optimization procedure to obtain the model parameters for each membrane. Through adjustment, A_w and B_s arise naturally from the results of J_w and J_s ; however K_s is a parameter that cannot be directly measured in experimental tests, and it is dependent on the membrane structural parameter (S) defined in Equation (8).

Table 2. Main parameters obtained by fitting the model to the experimental data.

Membrane	A_w ($\text{m}^2 \cdot \text{s} \cdot \text{kg}^{-1}$)	B_s ($\text{m} \cdot \text{s}^{-1}$)	K_s ($\text{s} \cdot \text{m}^{-1}$)
FTSH2O	1.29×10^{-12}	4.68×10^{-8}	2.88×10^5
HFFO2	2.17×10^{-12}	5.40×10^{-8}	1.60×10^5

The values of the permselective parameters obtained by fitting the model to the experimental data (Table 2) were compared to the values provided in the literature for each membrane. In the case of the FTSH2O membrane, the parameters A_w and B_s were 32.8% and 50.9% lower, respectively, than those obtained in Ref. [31] ($A_w = 1.92 \times 10^{-12} \text{ m}^2 \cdot \text{s}^{-1} \cdot \text{kg}^{-1}$ and $B_s = 9.44 \times 10^{-8} \text{ m} \cdot \text{s}^{-1}$). However, in the case of the HFFO2 membrane, the A_w parameter was 50.4% lower, but B_s was 20.9% higher, in comparison with the values obtained in Ref. [32] ($A_w = 4.427 \times 10^{-12} \text{ m}^2 \cdot \text{s}^{-1} \cdot \text{kg}^{-1}$ and $B_s = 4.17 \times 10^{-8} \text{ m} \cdot \text{s}^{-1}$). The differences in the parameter values were not very significant, but it was observed that the relationship between A_w and B_s changed in a different manner for each membrane, after fitting to the model proposed in this work. The difference could be due to the methodology used by the other authors to determine the parameters. The parameters for the FTSH2O membrane were determined following standard procedures [33,34], while for the HFFO2 membrane, the parameters were calculated using the modified model of Bui et al. [35] for randomly packed fiber bundles.

The use of different salts under the same operating conditions can generate different results for the parameters. Therefore, as Sanahuja-Embuena et al. [32] point out, the modeling method requires subjective judgment, and the calculated values should be treated as estimations.

4.2. Membrane Test and Model Predictions

Flux modeling is essential to predict how flux performance changes under varying system conditions or membrane structures. Using the model presented in Section 2, the results obtained with NaCl ($200 \text{ g} \cdot \text{L}^{-1}$) as the DS and distilled H_2O as the FS (Figures 4a and 5a), and those with NaCl ($30 \text{ g} \cdot \text{L}^{-1}$) as the DS and $1 \text{ g} \cdot \text{L}^{-1}$ tyrosol as the FS (Figures 4b and 5b) are shown for the FTSH2O (Figure 4) and HFFO2 (Figure 5) membranes.

For the system modeling study, the results obtained are presented again, but this time, the fitting was performed using data regarding the evolution of the volumes of the DS and FS (V_D and V_F , respectively) and the DS and FS concentrations (C_D and C_F , respectively) in the tank. This type of adjustment can be more accurate, since the temporal derivatives of the fluxes are very sensitive to disturbances, while the fitting based on a cumulative variable dampens the results. Additionally, to compare the flux predicted by the model and the experimental results, a moving average smoothing function was used for the flux.

In general, it can be seen in both Figures 4 and 5 that, after readjustment of the parameters, the volume, concentration and J_w trends are met. In both membranes, the values obtained for A_w and B_s were lower than those previously observed (Table 2). In addition, when tyrosol was present, these levels were even lower. This may be a consequence of the

tyrosol creating an additional layer of resistance that hinders the passage of water and salt. A more detailed study using a bilayer model could be attempted.

When working with model solutions that only contain tyrosol, there is no influence of fouling, due to the deposit of other solutes on the membrane surface. In this case, the decrease in J_w is mainly due to the decrease in the osmotic pressure over time, and is mainly due to dilutive ICP (a characteristic of asymmetric FO membranes) [36]. In other studies where a CTA membrane was used to treat OMW, ATR-FTIR analysis was used to characterize the membrane surface after the process. A characteristic peak around 1580 cm^{-1} was observed, which is attributable to the C–C stretching that occurs in the aromatic rings of polyphenols, demonstrating their adhesion to the surface of the membrane [37]. It is important to note that due to the almost total absence of hydraulic pressure in the FO operation, less compaction of the fouling layer occurs, thus facilitating the recovery of the membrane.

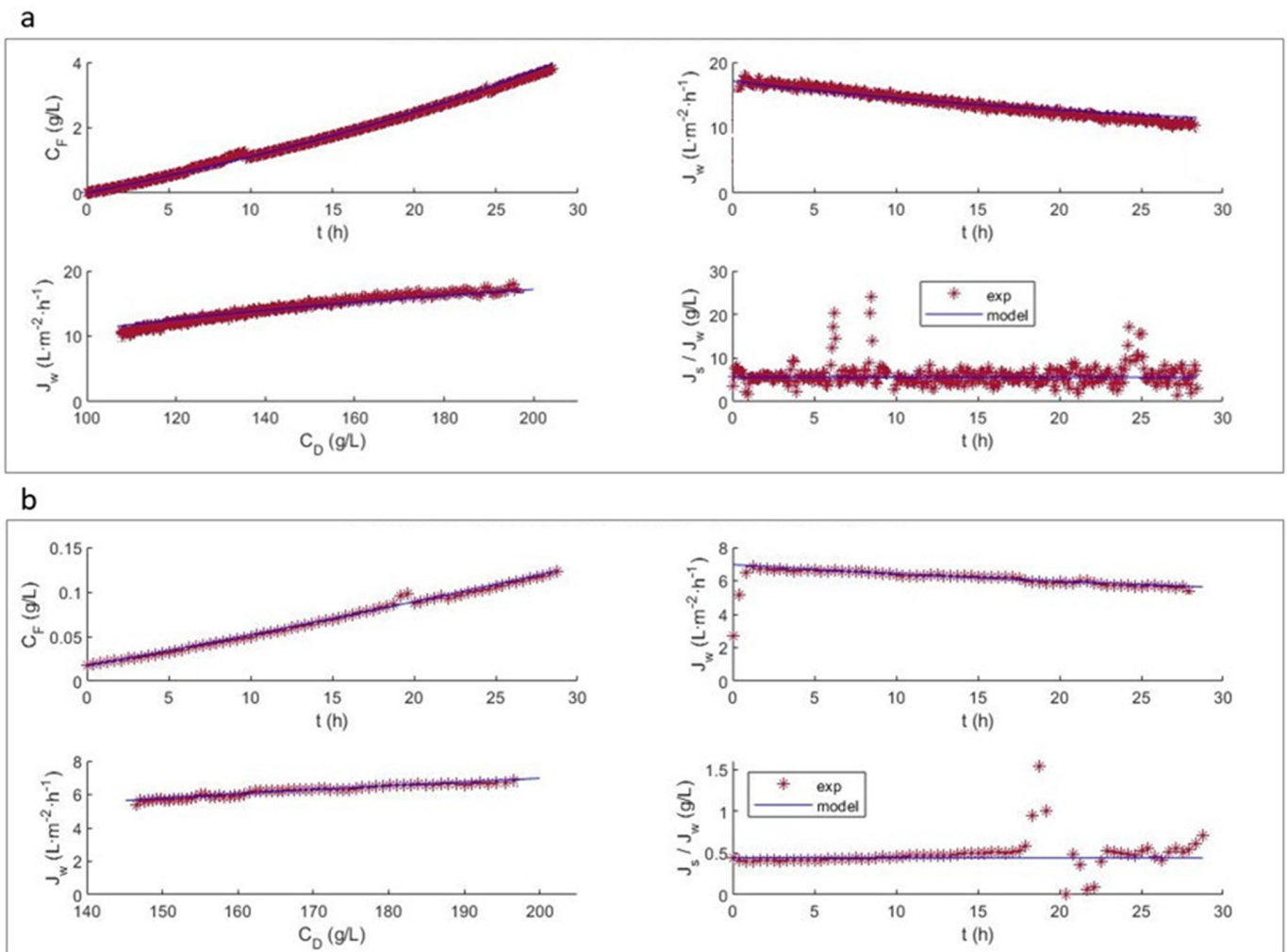


Figure 4. Comparison of experimental and predicted data for the FTSH2O membrane (a) test (i) with 200 g L^{-1} NaCl as the DS and distilled H_2O as the FS; (b) test (ii) with 30 g L^{-1} NaCl as the DS and 1 g L^{-1} tyrosol as the FS.

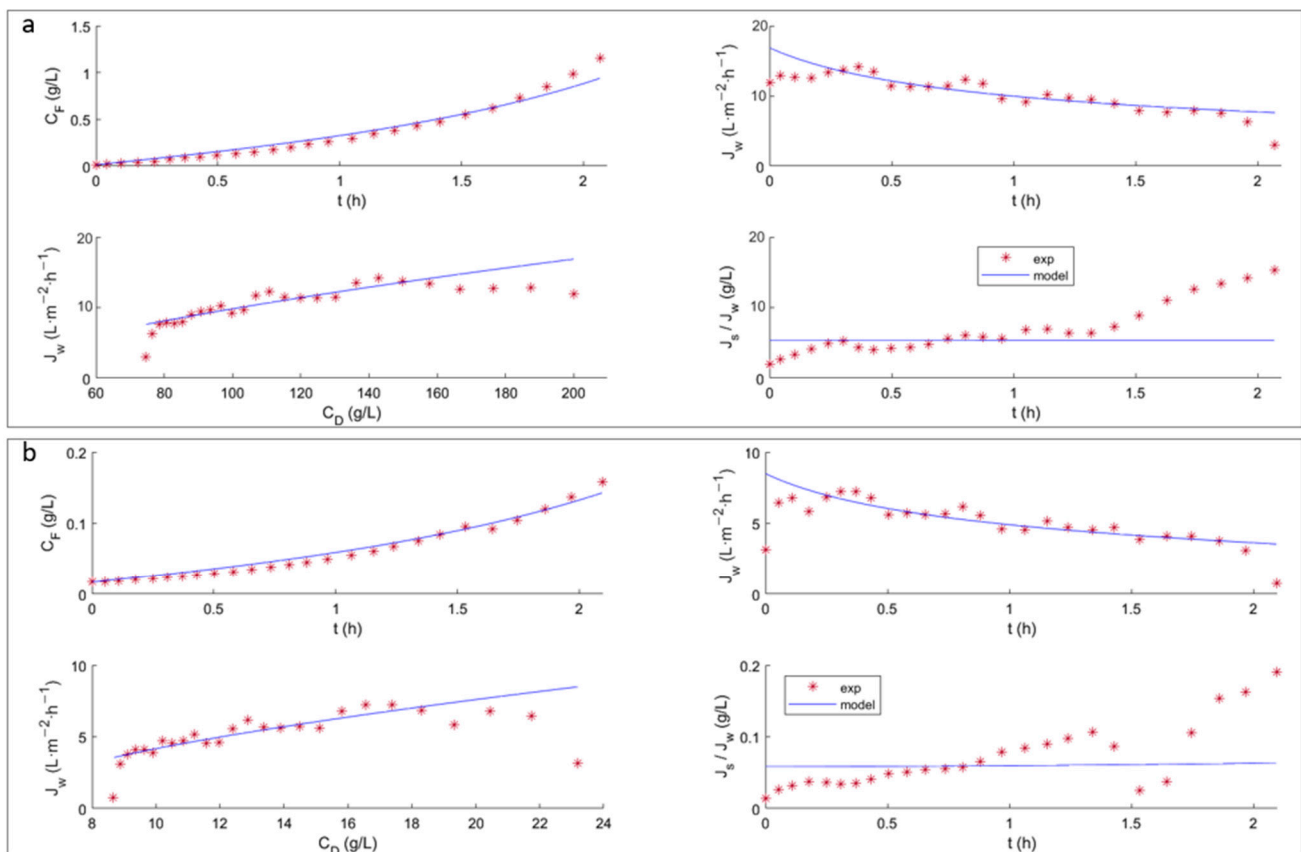


Figure 5. Comparison of experimental and predicted data for the HFFO2 membrane (a) test (i) with 200 g L^{-1} NaCl as the DS and distilled H_2O as the FS; (b) test (ii) with 30 g L^{-1} NaCl as the DS and 1 g L^{-1} tyrosol as the FS. The parameters were readjusted with respect to the original test using salt.

The effect of ECP and ICP on the determination of water flux can be observed. The reduction in flux is mainly attributed to the decrease in the osmotic pressure difference, with the impact of ICP and ECP not being significantly prominent for the test performed with distilled water as the FS (Figures 4a and 5a). However, the impact of ECP and ICP is more complex in the FS containing more foulants such as tyrosol, and it increases under high osmotic conditions (Figures 4b and 5b). It can also be observed that the flux of the FTSH2O membrane is more significantly influenced by both the difference in NaCl concentration in the DS and the presence of tyrosol in the FS, decreasing the initial flux by half. However, this was not observed with the HFFO2 membrane, which showed stable fluxes of similar values.

It was expected that, having obtained the parameters by testing in the absence of tyrosol, the model would better fit the results of test (i) compared to test (ii); however, this was not the case. It was observed that the parameters required significant readjustments for test (i) performed with the FTSH2O membrane (Figure 4a), even for the value of K_s . This may be because the tests presented in the previous section (Figure 2) and the test using tyrosol (Figure 4b) were performed with a different membrane coupon. However, this did not occur with the HFFO2 membrane, despite the fact that, as in the previous test, the salt assays of test (i) were performed with a new piece of membrane. This would imply a higher variability in the flat membrane than in the hollow fiber example. This could also explain the discrepancies between the mean evolution slope and experimental slope observed in the J_w subfigures. This confirms the manufacturing variability of this type of membrane.

It can be seen that the experimental J_s/J_w value for the flat membrane (Figure 4) presents a deviation from linearity between 18 and 22 h of testing. This is due to a change in the conductivity meter used to adapt to the conductivity values reached. Despite the

discontinuity observed, the model achieved a good representation of the information, without being affected by these anomalous data. For the HFFO2 membrane (Figure 5), it is again observed that the experimental J_s/J_w ratio increased with time, while according to the model, it should not vary as significantly and should be very similar to the A_w/B_s ratio. However, the ratio decreased with time and therefore, it also reduced along with the decrease in CD. This result therefore reinforces the previous hypothesis regarding a transient stabilization of the membrane behavior.

5. Conclusions

Most forward osmosis modeling approaches do not consider the concentration of components other than salt in the feed solution. It is even common not to consider the salt passage. In this work, salt passage and the effect of organics on osmotic pressure have been taken into account in the modeling, along with the existence of internal and external polarization layers.

The experimental results were obtained with a model solution that simulates olive mill wastewater, which included tyrosol as a solute. The experimental data was adjusted to the developed model, and it was possible to estimate the solvent and solute permeability parameters, as well as the polarization modulus, starting from values obtained in the literature and readjusting them.

The differences between the permselective parameters obtained after fitting the model to the experimental data and those found in the literature were not significant. However, for both membranes, the ratio between the solvent and the solute permeability coefficients was affected differently. The permeate flux levels predicted by the model were very close to the experimental values, especially in the case of the FTSH2O membrane.

In conclusion, the inclusion of the contribution of low molecular weight organic compounds to the osmotic pressure may contribute to a better estimation of the transport parameters of a forward osmosis process applied to real feed streams than estimations obtained using theoretical models that only consider the contribution of salts to osmotic pressure.

Author Contributions: Conceptualization, M.C.-C., S.Á.-B. and J.M.G.-Z.; methodology, M.C.-C. and J.M.G.-Z.; software, J.M.G.-Z.; validation, M.C.-C.; formal analysis, M.C.-C.; investigation, M.C.-C. and J.M.G.-Z.; resources, S.Á.-B., J.A.M.-R. and M.C.V.-V.; data curation, M.C.-C. and J.M.G.-Z.; writing—original draft preparation, M.C.-C. and J.M.G.-Z.; writing—review and editing, M.C.-C., S.Á.-B. and J.M.G.-Z.; visualization, M.C.-C., S.Á.-B. and J.M.G.-Z.; supervision, S.Á.-B., J.A.M.-R. and M.C.V.-V.; project administration, S.Á.-B., J.A.M.-R. and M.C.V.-V.; funding acquisition, S.Á.-B. and M.C.V.-V. All authors have read and agreed to the published version of the manuscript.

Funding: This research was funded by MCIN/AEI/10.13039/501100011033 and by ERDF, grant number CTM2017-88645-R, and the EU through the Operational Program FSE/ACIF-2018.

Institutional Review Board Statement: Not applicable.

Data Availability Statement: The raw data of this study are available on request.

Conflicts of Interest: The authors declare no conflict of interest. The funders had no role in the design of the study; in the collection, analyses, or interpretation of data; in the writing of the manuscript; or in the decision to publish the results.

References

1. Goh, P.S.; Ismail, A.F.; Ng, B.C.; Abdullah, M.S. Recent Progresses of Forward Osmosis Membranes Formulation and Design for Wastewater Treatment. *Water* **2019**, *11*, 2043. [[CrossRef](#)]
2. Bottino, A.; Capannelli, G.; Comite, A.; Costa, C.; Firpo, R.; Jezowska, A.; Pagliero, M. Treatment of Olive Mill Wastewater through Integrated Pressure-Driven Membrane Processes. *Membranes* **2020**, *10*, 334. [[CrossRef](#)]
3. Sánchez-Arévalo, C.M.; García-Serrano, A.P.; Vincent-Vela, M.C.; Álvarez-Blanco, S. Combining Ultrafiltration and Nanofiltration to Obtain a Concentrated Extract of Purified Polyphenols from Wet Olive Pomace. *Membranes* **2023**, *13*, 119. [[CrossRef](#)]
4. Cifuentes-Cabezas, M.; Sanchez-Arévalo, C.M.; Mendoza-Roca, J.A.; Vincent-Vela, M.C.; Álvarez-Blanco, S. Recovery of phenolic compounds from olive oil washing wastewater by adsorption/desorption process. *Sep. Purif. Technol.* **2022**, *298*, 121562. [[CrossRef](#)]

5. Blandin, G.; Ferrari, F.; Lesage, G.; Le-Clech, P.; Héran, M.; Martínez-Lladó, X. Forward Osmosis as Concentration Process: Review of Opportunities and Challenges. *Membranes* **2020**, *10*, 284. [[CrossRef](#)]
6. Sousa, M.R.S.; Lora-García, J.; López-Pérez, M.-F. Experimental study and modeling of forward osmosis process for activated sludge concentration by using residual brine from a stuffed olive factory as draw solution. *J. Water Process. Eng.* **2018**, *21*, 143–153. [[CrossRef](#)]
7. Tundis, R.; Conidi, C.; Loizzo, M.R.; Sicari, V.; Romeo, R.; Cassano, A. Concentration of Bioactive Phenolic Compounds in Olive Mill Wastewater by Direct Contact Membrane Distillation. *Molecules* **2021**, *26*, 1808. [[CrossRef](#)]
8. Haupt, A.; Lerch, A. Forward Osmosis Application in Manufacturing Industries: A Short Review. *Membranes* **2018**, *8*, 47. [[CrossRef](#)]
9. Suh, C.; Lee, S. Modeling reverse draw solute flux in forward osmosis with external concentration polarization in both sides of the draw and feed solution. *J. Membr. Sci.* **2013**, *427*, 365–374. [[CrossRef](#)]
10. Goi, Y.; Liang, Y.; Lau, W.; Weihs, G.F. Analysis of the effect of advanced FO spacer on the specific energy consumption of hybrid RO desalination system. *J. Membr. Sci.* **2023**, *668*, 121247. [[CrossRef](#)]
11. Yang, X.; Wang, S.; Hu, B.; Zhang, K.; He, Y. Estimation of concentration polarization in a fluidized bed reactor with Pd-based membranes via CFD approach. *J. Membr. Sci.* **2019**, *581*, 262–269. [[CrossRef](#)]
12. Ryu, H.; Mushtaq, A.; Park, E.; Kim, K.; Chang, Y.K.; Han, J.-I. Dynamical Modeling of Water Flux in Forward Osmosis with Multistage Operation and Sensitivity Analysis of Model Parameters. *Water* **2019**, *12*, 31. [[CrossRef](#)]
13. Singh, S.K.; Sharma, C.; Maiti, A. Modeling and experimental validation of forward osmosis process: Parameters selection, permeate flux prediction, and process optimization. *J. Membr. Sci.* **2023**, *672*, 121439. [[CrossRef](#)]
14. Lee, K.; Baker, R.; Lonsdale, H. Membranes for power generation by pressure-retarded osmosis. *J. Membr. Sci.* **1981**, *8*, 141–171. [[CrossRef](#)]
15. Loeb, S.; Titelman, L.; Korngold, E.; Freiman, J. Effect of porous support fabric on osmosis through a Loeb-Sourirajan type asymmetric membrane. *J. Membr. Sci.* **1997**, *129*, 243–249. [[CrossRef](#)]
16. Tang, C.Y.; She, Q.; Lay, W.C.L.; Wang, R.; Fane, A.G. Coupled effects of internal concentration polarization and fouling on flux behavior of forward osmosis membranes during humic acid filtration. *J. Membr. Sci.* **2010**, *354*, 123–133. [[CrossRef](#)]
17. Zhang, X.; Li, Q.; Wang, J.; Li, J.; Zhao, C.; Hou, D. Effects of feed solution pH and draw solution concentration on the performance of phenolic compounds removal in forward osmosis process. *J. Environ. Chem. Eng.* **2017**, *5*, 2508–2514. [[CrossRef](#)]
18. Li, J.; Liu, Q.; Liu, Y.; Xie, J. Development of electro-active forward osmosis membranes to remove phenolic compounds and reject salts. *Environ. Sci. Water Res. Technol.* **2016**, *3*, 139–146. [[CrossRef](#)]
19. McCutcheon, J.R.; Elimelech, M. Influence of concentrative and dilutive internal concentration polarization on flux behavior in forward osmosis. *J. Membr. Sci.* **2006**, *284*, 237–247. [[CrossRef](#)]
20. Tan, C.H.; Ng, H.Y. Modified models to predict flux behavior in forward osmosis in consideration of external and internal concentration polarizations. *J. Membr. Sci.* **2008**, *324*, 209–219. [[CrossRef](#)]
21. Haupt, A.; Marx, C.; Lerch, A. Modelling Forward Osmosis Treatment of Automobile Wastewaters. *Membranes* **2019**, *9*, 106. [[CrossRef](#)] [[PubMed](#)]
22. Li, X.; He, T.; Dou, P.; Zhao, S. 2.5 Forward Osmosis and Forward Osmosis Membranes. *Compr. Membr. Sci. Eng.* **2017**, *2*, 95–123. [[CrossRef](#)]
23. Gu, B.; Kim, D.; Kim, J.; Yang, D. Mathematical model of flat sheet membrane modules for FO process: Plate-and-frame module and spiral-wound module. *J. Membr. Sci.* **2011**, *379*, 403–415. [[CrossRef](#)]
24. Nagy, E.; Hegedüs, I.; Rehman, D.; Wei, Q.J.; Ahdab, Y.D.; Lienhard, J.H. The Need for Accurate Osmotic Pressure and Mass Transfer Resistances in Modeling Osmotically Driven Membrane Processes. *Membranes* **2021**, *11*, 128. [[CrossRef](#)]
25. Cifuentes-Cabezas, M.; Carbonell-Alcaina, C.; Vincent-Vela, M.C.; Mendoza-Roca, J.A.; Álvarez-Blanco, S. Comparison of different ultrafiltration membranes as first step for the recovery of phenolic compounds from olive-oil washing wastewater. *Process. Saf. Environ. Prot.* **2021**, *149*, 724–734. [[CrossRef](#)]
26. Salamanca, M.; López-Serna, R.; Palacio, L.; Hernandez, A.; Prádanos, P.; Peña, M. Ecological Risk Evaluation and Removal of Emerging Pollutants in Urban Wastewater by a Hollow Fiber Forward Osmosis Membrane. *Membranes* **2022**, *12*, 293. [[CrossRef](#)]
27. Luján-Facundo, M.; Mendoza-Roca, J.; Soler-Cabezas, J.; Bes-Piá, A.; Vincent-Vela, M.; Cuartas-Urbe, B.; Pastor-Alcañiz, L. Management of table olive processing wastewater by an osmotic membrane bioreactor process. *Sep. Purif. Technol.* **2020**, *248*, 117075. [[CrossRef](#)]
28. Liang, Y.; Fletcher, D. Computational fluid dynamics simulation of forward osmosis (FO) membrane systems: Methodology, state of art, challenges and opportunities. *Desalination* **2023**, *549*, 116359. [[CrossRef](#)]
29. Cifuentes-Cabezas, M.; Pavani, A.; Vincent-Vela, M.C.; Mendoza-Roca, J.A.; Álvarez-Blanco, S. Concentration of phenolic compounds from olive washing wastewater by forward osmosis using table olive fermentation brine as draw solution. *Environ. Technol. Innov.* **2023**, *30*, 103054. [[CrossRef](#)]
30. Singleton, V.L.; Orthofer, R.; Lamuela-Raventós, R.M. Analysis of total phenols and other oxidation substrates and antioxidants by means of folin-ciocalteu reagent. *Methods Enzymol.* **1999**, *299*, 152–178.
31. Madsen, H.T.; Nissen, S.S.; Muff, J.; Søgaard, E.G. Pressure retarded osmosis from hypersaline solutions: Investigating commercial FO membranes at high pressures. *Desalination* **2017**, *420*, 183–190. [[CrossRef](#)]

32. Sanahuja-Embuena, V.; Khensir, G.; Yusuf, M.; Andersen, M.F.; Nguyen, X.T.; Trzaskus, K.; Pinelo, M.; Helix-Nielsen, C. Role of Operating Conditions in a Pilot Scale Investigation of Hollow Fiber Forward Osmosis Membrane Modules. *Membranes* **2019**, *9*, 66. [[CrossRef](#)] [[PubMed](#)]
33. Cath, T.Y.; Elimelech, M.; McCutcheon, J.R.; McGinnis, R.L.; Achilli, A.; Anastasio, D.; Brady, A.R.; Childress, A.E.; Farr, I.V.; Hancock, N.T.; et al. Standard Methodology for Evaluating Membrane Performance in Osmotically Driven Membrane Processes. *Desalination* **2013**, *312*, 31–38. [[CrossRef](#)]
34. Kim, Y.C.; Lee, J.H.; Park, S.-J. Novel crossflow membrane cell with asymmetric channels: Design and pressure-retarded osmosis performance test. *J. Membr. Sci.* **2015**, *476*, 76–86. [[CrossRef](#)]
35. Bui, N.-N.; Arena, J.T.; McCutcheon, J.R. Proper accounting of mass transfer resistances in forward osmosis: Improving the accuracy of model predictions of structural parameter. *J. Membr. Sci.* **2015**, *492*, 289–302. [[CrossRef](#)]
36. Singh, S.K.; Sharma, C.; Maiti, A. A comprehensive review of standalone and hybrid forward osmosis for water treatment: Membranes and recovery strategies of draw solutions. *J. Environ. Chem. Eng.* **2021**, *9*, 105473. [[CrossRef](#)]
37. Gebreyohannes, A.Y.; Curcio, E.; Poerio, T.; Mazzei, R.; Di Profio, G.; Drioli, E.; Giorno, L. Treatment of Olive Mill Wastewater by Forward Osmosis. *Sep. Purif. Technol.* **2015**, *147*, 292–302. [[CrossRef](#)]

Disclaimer/Publisher's Note: The statements, opinions and data contained in all publications are solely those of the individual author(s) and contributor(s) and not of MDPI and/or the editor(s). MDPI and/or the editor(s) disclaim responsibility for any injury to people or property resulting from any ideas, methods, instructions or products referred to in the content.